INTRODUCTION OF A REALTIME DIESEL-ENGINE MODEL FOR CONTROLLER DESIGN

Dara D. Torkzadeh, Uwe Kiencke

Institute of Industrial Information Technology,
University of Karlsruhe, D-76187 Karlsruhe, Germany
E-Mail: torkzadeh@iiit.etec.uni-karlsruhe.de and
kiencke@iiit.etec.uni-karlsruhe.de

Abstract: Diesel engines with direct injection have become very important in recent years. Because of flexible injection curves, the energy conversion can be manipulated during operation. To examine how the pressure inside the combustion chamber is influenced new engine models are necessary.
The engine model introduced in this paper can be used in the development process of engine control units and as a state observer for sophisticated controllers during on-board operation of the car. This paper provides a brief introduction into the model, indicating problems and solutions involved in realtime calculation.

1. INTRODUCTION

In recent years, direct-injecting diesel engines have become more and more important for the automobile industry. The advantages of these types of engines lie in a good fuel economy combined with high power output.

Common-rail systems allow to shape the injection curve as necessary. It is possible to establish a pre-, main- and post-injection or even multiple injections. Furthermore, every type of injection curve can be applied. Due to flexibility in injection curve, the energy conversion process has to be calculated in a flexible way. The Vibe- or Double-Vibe [1] functions formerly used as an approximation for the energy conversion process cannot be employed any longer.

In this paper, a phenomenological approach for evaporation is used as input to the thermodynamic equations involved. Thus, influence of the injection curve on pressure and temperature inside the combustion chamber can be derived. The information on in-cylinder variables can be taken as input for several sophisticated controllers than applied in ECU's [2] today. For usage during on-board operation, the combustion process has to be calculated in realtime.

In this project, different engine models have been designed for various fields of applications. There is a model of a single cylinder for realtime calculation as well as a four-cylinder model of the complete engine including frictional forces. The four-cylinder model is used in functionality development to examine controllers in an early stage of the development process in order to save costs. Another idea for the engine model is to fit stricter emission laws by changing the shape of the injection curve. For this purpose, an emission model may be used (Torkzadeh *et al.*, 2001).

As a first part, the paper will explain the structure of the model. Reflecting the importance, next an evaporation model is presented. The problems and solutions invoked by realtime calculation will be discussed. Finally, exemplary results of the model are presented.

2. MODEL STRUCTURE

In this section the structure of the engine model will be explained. Figure 1 gives a conceptional overview of the different models, designed as part of this project. The injection-rate and the idle-speed serve as input to the model. Further models may be connected to the

---

[1] For more information see (Pischinger and KraSSnig, 1989).
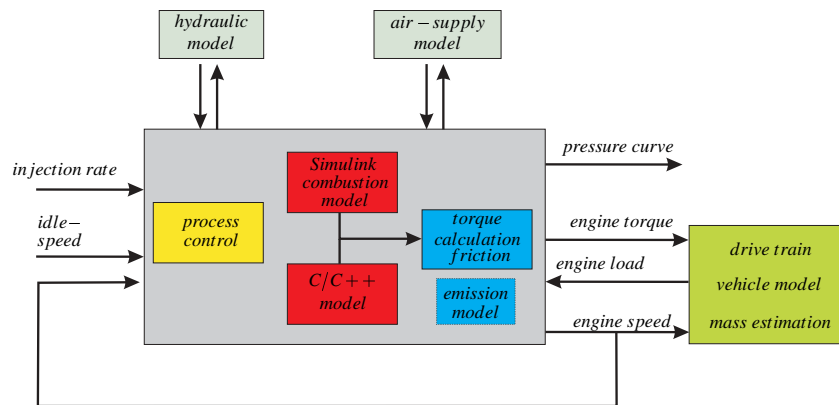[2] ECU = engine control unit

Fig. 1. Structure of the engine-model-toolbox.

engine model via interfaces, e.g. a hydraulic model of the common-rail itself or a model for the intake and outlet air-ways.

Included in the model is a central unit for process-control. The combustion model itself is provided in two modelling languages: Matlab/Simulink and C/C++. The reasons will be explained later on (see paragraph 4). Another unit is responsible for the calculation of engine friction and, with help of crankshaft geometry, as output signal the engine torque. In addition, an emission-model for *NOx* and *OCH* is available. Due to extremely complex chemical reactions, these emissions cannot be calculated in realtime.
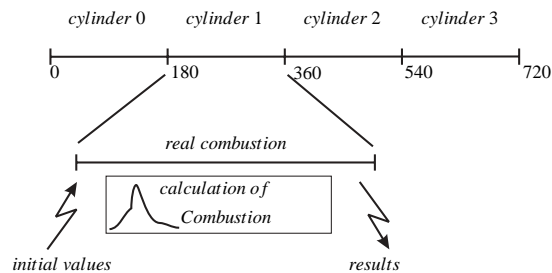

Fig. 2. Model in realtime environment.

Engine-speed, engine-torque, pressure and temperature are the output signals of the model. With an engine-speed feedback, the model may run autonomously except for single input injection-rate. A drivetrain model can be connected to the output to simulate the complete powertrain section.

To adapt the model to real engine conditions, all important engine parameters are adaptable. Example are drill, upstroke, crankshaft geometry, number of drills of the injector and so on. Furthermore, some parameters can be changed dynamically, during simulation, e.g. EGR [3] -rate, fuel pressure inside the common-rail or turbo-charge pressure. The degree of freedom of the model is 34.

Figure 2 shows the implementation of the model into a real car environment. The model receives initial values from the ECU via CAN [4] -bus. With help of this information, a single combustion is calculated. The results may optionally be sent back to the ECU, via CAN-bus. Because of a four-cylinder engine, a crankshaft angle of 180° only is available for a single combustion simulation. To save resources, the combustion process itself is built once. Each time an crankshaft angle of 180° is reached, the model calculates all important variables in parallel to the real combustion process.

3. EVAPORATION AND COMBUSTION MODEL

In this section a short introduction of the evaporation model and the thermodynamics will be presented.

3.1 *Evaporation*

Modern diesel engines with a common rail injection system can use many different forms of injection curves, as explained in section 1. For realistic simulation results and a flexible simulation, the fuel spray model of Constien (Constien, 1991) is used. The fuel spray model is a basic approach that calculates a phenomenological burning function according to a given injection curve.

The injection is controlled by an injection-curve. Along this curve, fuel is injected into the virtual combustion chamber over the crankshaft angle. For every injected fuel portion the amount of liquid, gaseous and burned components will be determined as function of the crankshaft angle. Figure 3 shows the different states of the fuel portions injected at different crankshaft angles.

As it is impossible to analytically describe the multitude of drop diameters, an average drop diameter dependent from injection pressure and from mass

---

[3] EGR = exhaust gas recirculation, used to avoid emissions
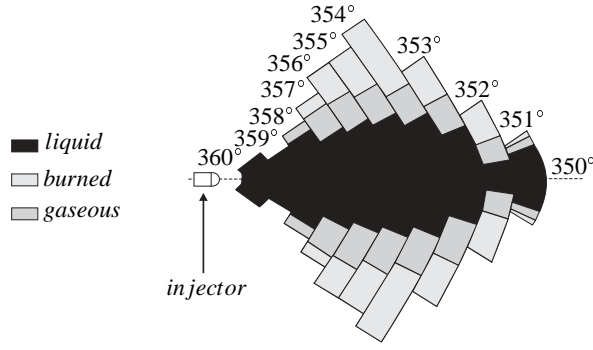
[4] CAN = Controller Area Network

Fig. 3. Fuel Spray Model

of the fuel portion is adopted according the Sauter (Constien, 1991) approach:

$$d_{32} = \frac{\sum_i d_{Ti}^3 \cdot H_i}{\sum_i d_{Ti}^2 \cdot H_i} \quad . \tag{1}$$

H is the number of drops with identical diameter, d_T is the drop diameter and i represents the injection time. To calculate the Sauter diameter d_{32} the Varde/Popa/Varde (Herzog, 1989) approach is used:

$$d_{32} = 16.58 \left(Re \cdot We \right)^{-0.28} \quad , \tag{2}$$

where Re is the Reynolds number and We the Weber number of the flow. The Sauter diameter finally is calculated in dependence of air density ρ_L, fuel density ρ_K, fuel surface strain σ_K, kinetic fuel viscosity ϑ_K and diameter of the injector nozzle d_T:

$$d_{32} = 12.392 \cdot \frac{d_T^{0.44} \cdot \rho_K^{0.42} \cdot (\sigma_K \cdot \vartheta_K)^{0.28}}{\Delta p^{0.42} \cdot \rho_L^{0.28}} \quad . \tag{3}$$

Furthermore, the number of drops $N_{T,i}$ as function of injected fuel portion $m_{K,i}$ is required to compute the evaporation:

$$N_{T,i} = \frac{m_{K,i}}{\frac{\pi}{6} \cdot d_{32}^3 \cdot \rho_K} \quad . \tag{4}$$

By means of equations 2 and 4, the surface $A_{K,i}$ of all drops accrued in time step i can be calculated:

$$A_{K,i} = N_{T,i} \cdot \pi \cdot d_{32}^3 \quad . \tag{5}$$

Finally, the amount of fuel $m_{K,V,i}$ evaporating in every time step can be calculated in dependence of drop diameter d_{32}, surface $A_{K,i}$, in cylinder pressure p, engine speed n and a diffusion constant C_{Diff}:

$$m_{K,V,i} = C_{Diff} \cdot A_{K,i} \cdot p^{m_p} \cdot \frac{1}{60 \cdot n \cdot d_{32}} \quad . \tag{6}$$

The amount of liquid fuel at the next step $i+1$ is calculated by subtracting the evaporating fuel of equation 6 from the liquid proportion of the last step i

$$m_{K,i+1} = m_{K,i} - m_{K,V,i} \quad . \tag{7}$$

The drop diameter d_T needs to be determined in every time step:

$$d_{T,i} = \sqrt[3]{\frac{m_{K,i}}{\frac{\pi}{6} \cdot N_{T,i}}} \quad . \tag{8}$$

The inflammation delay time τ_{ZV} is calculated with an empirical formula used by Constien (Constien, 1991):

$$\tau_{ZV} = 2.1 \cdot \overline{p}^{-1.02} \cdot e^{\frac{2100K}{\overline{T}}} \quad , \tag{9}$$

where $\overline{p}$ represents the mean pressure and $\overline{T}$ the mean temperature for a given time interval.

3.2 Combustion

The basis for the combustion model is a two-zone model, with one zone filled with fresh air and the other zone filled with the combustion products. For the simulation the same pressure is assumed throughout the whole combustion chamber. Furthermore, the mixture meant to be homogeneous inside each zone. There is no simulation of swirl- or blow-by effects.

For the calculation of the combustion process itself, the thermodynamic equation for the combustion chamber has to be solved:

$$dW_t + dQ_a + \sum_i dm_i \cdot (h_i + e_{ai})$$
$$= dU + dE_a \tag{10}$$

where W_t is technical work, Q_a external heat, m_i mass crossing the system border with the enthalpy h_i and specific external energy e_{ai}. U is the internal energy of the system, E_a the external energy e.g. kinetic or potential energy. In addition, the flame process and the air-fuel ratio in the flame front have to be derived.

After charge exchange, fuel injection and evaporation process start, being calculated as described above. As soon as the cylinder temperature is high enough and inflammation delay time is expired, the combustion process will begin in the flame front. The combustion process may already have started while fuel is still being injected. The mass air flow from the unburned area through the flame front into the burned area has to be calculated. The volume of the unburned area decreases and the one of the burned area increases until the entire combustion chamber is filled with burned gas and the combustion ends.

The instantaneous air-fuel ratio λ_V in the combusted zone results from following equation:

$$\lambda_V = \frac{m_V - m_B - m_{Br}}{L_{st} \cdot (m_B + m_{Br})} \quad , \tag{11}$$

where m_V is mass of the burned mixture, m_B total amount of burned fuel, m_{Br} residual gas of the burned area and L_{st} stoichiometric air-fuel ratio.

The air-fuel ratio λ_i in the flame front represents how much fuel and air merge out of the unburned zone into the flame front to be burned. The evaporation model yields the input values for the flame front. In diesel engines, the inflammation starts first with a rich mixture getting leaner during the combustion. A definition of the air-fuel ration λ_i in the flame front can be found in (Pischinger and KraSSnig, 1989):

$$\lambda_i = \frac{\frac{dm_V}{d\varphi} - \frac{dm_B}{d\varphi} - \frac{dm_{Br}}{d\varphi}}{L_{st} \cdot \left(\frac{dm_B}{d\varphi} + \frac{dm_{Br}}{d\varphi} \right)} \quad . \tag{12}$$

According to the mass- and energy-balance of the two-dimensional model, the pressure change in the combustion chamber may now be derived (cp. equation 10). The following simplifications (Hohlbaum, 1992) were established for simulation:

$$\frac{\partial u_V}{\partial p} = \frac{\partial R_V}{\partial T_V} = \frac{\partial R_V}{\partial p} = \frac{\partial R_V}{\partial \lambda_V} = 0 \quad . \tag{13}$$

This simplification is applied because it has not been possible to solve the dependence from the internal energy u on the pressure and from the ideal gas constant R_V on pressure, temperature and air-fuel ratio.

In order to solve equation 10, the masses of the burned and unburned areas are necessary. The mass change dm_u of the unburned area is

$$\frac{dm_u}{d\varphi} = m \cdot \left(\frac{\frac{dm_{inj}}{d\varphi} - (1 + \lambda_i \cdot L_{st}) \cdot \frac{dm_B}{d\varphi}}{m - m_{R0} \cdot (1 + \lambda_i \cdot L_{st})} \right) \quad , \tag{14}$$

the mass change of the burned area is

$$\frac{dm_V}{d\varphi} = (1 + \lambda_i \cdot L_{st}) \cdot$$
$$\frac{m \cdot \frac{dm_B}{d\varphi} - m_{R0} \cdot \frac{dm_{inj}}{d\varphi}}{m - m_{R0} \cdot (1 + \lambda_i \cdot L_{st})} \tag{15}$$

in dependence from injected fuel mass m_{inj} and from mass of residual gas m_{R0} within the combustion chamber. The volume of the unburned area V_U can be calculated, considering specific heat capacity c_{vu} and heat loss Q_{Wu} throughout the covered combustion chamber wall by the unburned area:

$$\frac{dV_U}{d\varphi} = \frac{-\lambda_i \cdot L_{st}}{p \cdot \left(1 + \frac{c_{vu}}{R} \right)} \cdot T_V \cdot (c_{vu} + R)$$
$$\cdot \frac{m}{m - m_{Br} \cdot (1 + \lambda_i \cdot L_{st})} \cdot \frac{dm_B}{d\varphi}$$
$$- \frac{c_{vu} \cdot V_u}{R} \cdot \frac{dp}{d\varphi} - \frac{dQ_{Wu}}{d\varphi} \quad . \tag{16}$$

With equation 16, the volume of the burned area V_{Br} is now determinable:

$$V_{CC}(\varphi) = V_U + V_{Br} \quad . \tag{17}$$

The volume of the flame front V_x mab be derived as follows:

$$V_x = \frac{\left(m_V^{(n)} - m_V^{(n+1)} \right) \cdot R_m \cdot T_V}{10^5 \frac{N}{m^2 \cdot bar} \cdot p_Z} \quad , \tag{18}$$

where $m_V^{(n)}$ is the mass of the burned area in step n and p_Z the combustion chamber pressure.

4. REALTIME CALCULATION

In order to get satisfying results, it is necessary to provide a resolution, in terms of crankshaft angle, of at least 1°. This means for an engine speed of 3000 rpm a step size of at least $56\mu s$. Due to a very computational model, some precautions have to be made.

Figure 4 gives an overview of the model structure in realtime environment. The hardware used in this project is a so-called $alpha - combo$ from dSpace [5]. The alpha-combo includes two controllers, a Texas Instrument signal processor and a DEC-alpha processor. The alpha-combo is connected to the ECU via CAN-bus.
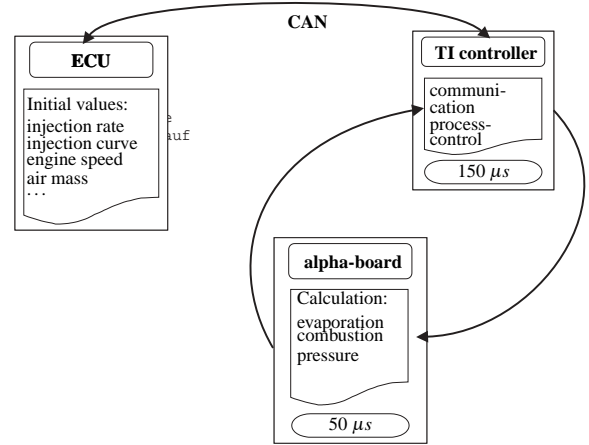

Fig. 4. Schematic structure of realtime environment.

The Texas Instruments controller is performing communication and process control. The calculation of evaporation and energy conversion is implemented on the alpha-controller. Via CAN-bus information about the injection rate, engine speed etc. are received from the ECU. Because of problems with the transmission ratio of the CAN-bus, the two controllers are forced to work with different step sizes.

To decrease step size on the alpha-controller several precautions have been taken:

- Avoidance of divisions. Divisions need more calculation power than multiplications.
- Simplification of the structure. The idea is to avoid multiple calculations of variables.

_____

[5] dSpace GmbH, Paderborn, Germany.

- Inclusion of optimized C/C++ code. With help of C/C++ code step size shall be decreased.

The results developed from these precautions have to be contemplated from different points of view. It has been possible to enhance performance on a PC and to increase robustness of the simulation. On a Pentium III with 1 GHz clock frequency realtime operation was almost possible.

On the other hand, the step size on the dSpace environment decreased from 100 μs to disappointing 90 μs only. Therefore, more effective precautions are required for acceleration of the simulation. An inspection of the model showed that the evaporation process contains a computationally inefficient loop, which calculates the surface of evaporated fuel. This loop contains following equations

$$SMD(\varphi_i) = \sqrt[3]{\frac{M_{ESV(post)}(\varphi_i)}{\frac{\pi}{6} \cdot n_{drp}(\varphi_i) \cdot \rho_{fuel}}} \qquad (19)$$

$$\Theta_i = n_{drp}(\varphi_i) \cdot \pi \cdot SMD(\varphi_i) \qquad (20)$$

$$\Delta m_{Dpf,i} = C_{Diff} \cdot \Theta_i \cdot p_z^{-1.09}(\varphi_i) \cdot$$
$$\frac{1}{SMD(\varphi_i) \cdot n_{eng}} \qquad (21)$$

$$\tau_{ZV} = 0.6 \cdot 3.45 \cdot 10^{-3} \cdot \overline{p}_Z^{-1.02} \cdot e^{\frac{2100}{T_Z}} \qquad (22)$$

for the Sauter diameter (equ. 19), the drop surface (equ. 20), the evaporated mass (equ. 21) and the ignition delay time (equ. 22). Those equations have to be calculated for every injected fuel portion in every time step of the simulation.

Because of power and root operations, evaluation of this loop is extremely slowing down the simulation. The DEC-alpha controller needs approximately 550 processor cycles to calculate a single power operation. To solve this problem, a Taylor approximation of the power and root operations was made. The Taylor approximation for $x^{-1.02}$, cp. equ. 22, as implemented in the model is exemplary presented in the following equations. This distinguish 3 different Taylor expansions as a result from different expansion environments:

$$x \leq 20$$
$$T(x) = 0.0632 - 4.2943 \cdot 10^{-3} \cdot (x - 15) +$$
$$2.8915 \cdot 10^{-4} \cdot (x - 15)^2 -$$
$$1.9405 \cdot 10^{-5} \cdot (x - 15)^3 \qquad (23)$$

$$20 < x \leq 70$$
$$T(x) = 0.0185 - 3.7729 \cdot 10^{-4} \cdot (x - 50) +$$
$$7.6214 \cdot 10^{-6} \cdot (x - 50)^2 -$$
$$1.5344 \cdot 10^{-7} \cdot (x - 50)^3 \qquad (24)$$

$$70 < x$$
$$T(x) = 0.0091 - 9.3025 \cdot 10^{-5} \cdot (x - 100) +$$
$$9.3955 \cdot 10^{-7} \cdot (x - 100)^2 -$$

$$9.4582 \cdot 10^{-9} \cdot (x - 100)^3 \ . \qquad (25)$$

With help of the Taylor approximation plus substitution of power operation by multiplication, it has been possible to reduce the step size to nearly 50 μs. The modified model may now simulate the combustion process of a diesel engine up to $\sim$ 3500 crankshaft revolutions per minute in realtime.

For a further decrease of step size, other approximations, like Tschebyscheff approximation are possible, due to their ability to minimize the computational effort with fewer multiplication operations. Another option is to include look-up tables for power and root operations. This subject of further development steps.

5. RESULTS

The designed engine has a displacement volume of 490 ccm per cylinder (10 cm upstroke, 7.9 cm drill). The injection pressure is 800 bar and includes a pre-injection. The engine simulation is executed for idle-speed condition with approximately 960 crankshaft revolutions per minute.
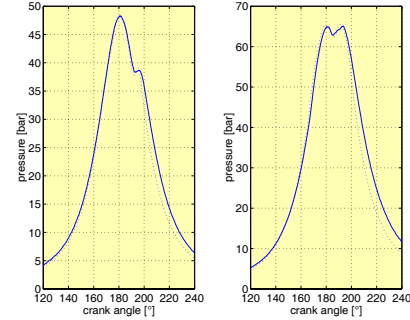

Fig. 5. Comparison of measured pressure data (solid) and simulation results (dashed).

Figure 5 shows the comparison between measured pressure data of an engine test bench and simulation results. It is obvious, that the calculated pressure curves nearly fits to the measured data when using identical boundary conditions. The model was adjusted by allying real engine parameters.

Figure 6 shows exemplary results of the Matlab/Simulink model. The model contains a unit to calculate frictional forces and the geometry of the crankshaft. A simple PI-controller is used in order to control the desired engine speed and to hold engine speed if there are changes on engine load. The PI-controller is not the most appropriate controller in this case, it was suitable for usage in the model.

The upper plot of figure 6 displays engine speed (in revolutions per minute), the lower one engine torque and mean torque per combustion cycle. The engine was working with an engine load of 100 Nm. As it can be seen, several changes of the engine speed where applied during simulation. To reach the desired engine

speed, the torque of the engine has changed. Torque and engine speed are oscillating as there is no flywheel or gearbox in the model implemented to smooth the torque and engine speed so far.
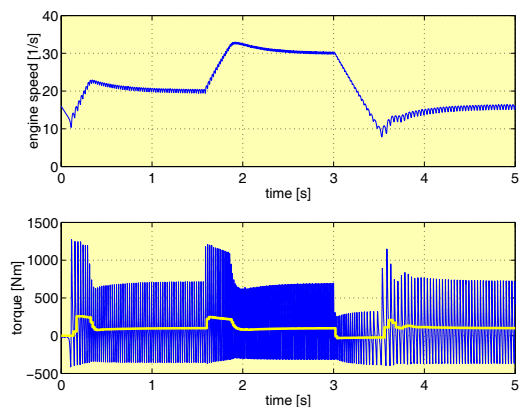

Fig. 6. Results of 4 cylinder engine model.

6. SUMMARY AND OUTLOOK

In this project different engine models for ECU development and realtime calculation have been designed. All models have the advantage of a flexible energy conversion function for future applications and injection curves. The phenomenological fuel-spray model is the central element of all models.

With help of the realtime model it is possible to calculate in-cylinder variables and use them as input for sophisticated controllers. The realtime model of the combustion process can be employed as state observer. The Matlab/Simulink models are suitable to simulate the complete engine, including frictional forces and crankshaft geometry. Interfaces allow the extension of the model, e.g. with a drivetrain model or a hydraulic model of the common-rail itself. This model can be applied in ECU-development for time- and cost-effectiveness.

In order to increase the performance of the model more precautions to simplify the computational effort have still to be found while not decreasing the quality of the results. In a next step, the realtime model may serve as state observer, during operation. Furthermore, with help of a drivetrain model, the simulation of the complete powertrain may be achievable in realtime .

7. REFERENCES

Constien, M. (1991). Bestimmung von Einspritz- und Brennverlauf eines direkt einspritzenden Dieselmotors. PhD thesis. Technische Universität München.

Herzog, P. (1989). *Möglichkeiten, Grenzen und Vorausberechnung der einspritzspezifischen Gemischbildung bei schnellaufenden Dieselmotoren mit direkter luftverteilender Kraftstoffeinspritzung.* Vol. 127 of *VDI Fortschrittberichte, Reihe 12, Verkehrstechnik/Fahrzeugtechnik,.* Düsseldorf.

Hohlbaum, B. (1992). Beitrag zur rechnerischen Untersuchung der Stickstoffoxid-Bildung schnellaufender Hochleistungsdieselmotoren. PhD thesis. Universität Karlsruhe.

Kiencke, U. and L. Nielsen (2000). *Automotive Control Systems*. Springer Verlag. Berlin, Heidelberg, New York.

Pischinger, R. and G. KraSSnig (1989). *Thermodynamik der Verbrennungskraftmaschine*. Vol. 5 of *Die Verbrennungskraftmaschine*. Springer Verlag. Berlin, Heidelberg, New York.

Torkzadeh, D., W. Längst and U. Kiencke (2001). Combustion and exhaust gas modeling of a common rail diesel engine - an approach. *SAE Paper*.

ANNOTATION